Pulse-by-pulse multi-beam-line operation for x-ray free-electron lasers

Toru Hara,[1,*] Kenji Fukami,[2] Takahiro Inagaki,[1] Hideaki Kawaguchi,[3] Ryota Kinjo,[1] Chikara Kondo,[1] Yuji Otake,[1] Yasuyuki Tajiri,[4] Hideki Takebe,[1,†] Kazuaki Togawa,[1] Tatsuya Yoshino,[3] Hitoshi Tanaka,[1] and Tetsuya Ishikawa[1]

[1]*RIKEN SPring-8 Center, Kouto 1-1-1, Sayo, Hyogo 679-5148, Japan*
[2]*Japan Synchrotron Radiation Research Institute, Kouto 1-1-1, Sayo, Hyogo 679-5198, Japan*
[3]*Nichicon Kusatsu Corporation, Yagura 2-3-1, Kusatsu, Shiga 525-0053, Japan*
[4]*SPring-8 Service Co., Ltd., Kouto 1-20-5, Shingu-cho, Tatsuno, Hyogo 679-5165, Japan*

(Received 31 August 2015; published 16 February 2016)

The parallel operation of plural undulator beam lines is an important means of improving the efficiency and usability of x-ray free-electron laser facilities. After the installation of a second undulator beam line (BL2) at SPring-8 Angstrom compact free-electron laser (SACLA), pulse-by-pulse switching between two beam lines was tested using kicker and dc twin-septum magnets. To maintain a compact size, all undulator beam lines at SACLA are designed to be placed within the same undulator hall located downstream of the accelerator. In order to ensure broad tunability of the laser wavelength, the electron bunches are accelerated to different beam energies optimized for the wavelengths of each beam line. In the demonstration, the 30 Hz electron beam was alternately deflected to two beam lines and simultaneous lasing was achieved with 15 Hz at each beam line. Since the electron beam was deflected twice by 3° in a dogleg to BL2, the coherent synchrotron radiation (CSR) effects became non-negligible. Currently in a wavelength range of 4–10 keV, a laser pulse energy of 100–150 μJ can be obtained with a reduced peak current of around 1 kA by alleviating the CSR effects. This paper reports the results and operational issues related to the multi-beam-line operation of SACLA.

DOI: 10.1103/PhysRevAccelBeams.19.020703

I. INTRODUCTION

X-ray free-electron lasers (XFELs), which are characterized by high peak intensity, short pulse duration, and coherence, have contributed to many brilliant outcomes across a variety of scientific fields, including biology, chemistry, material science, and nonlinear physics [1,2]. However, despite rapidly growing demand for XFELs, the number of facilities and experimental stations are still quite limited.

Since XFELs require high-brightness electron beams, a linear accelerator is used as an electron beam driver. Therefore, XFELs are effectively single-user facilities, which is a drawback compared to storage ring based synchrotron radiation facilities. To increase the capacity of experimental stations, XFEL facilities around the world have pursued multi-beam-line operation, in which the electron beam is distributed alternately to different beam lines on a bunch-to-bunch basis [3–5].

In the multi-beam-line design for XFELs, the undulator beam lines of long wavelengths conventionally branch off from the middle of the accelerator, where the electron beam energy remains low. However, this branching design requires additional undulator and experimental halls. At SPring-8 Angstrom compact free-electron laser (SACLA), all undulator beam lines are placed in the same undulator hall lying downstream from the accelerator to keep the facility compact. Instead, the final beam energies at the end of the accelerator are controlled from bunch to bunch to obtain a wide spectral range [6].

This paper describes the results of the multi-beam-line operation of SACLA and emerging issues related to coherent synchrotron radiation (CSR) [7].

II. MULTI-BEAM-LINE OPERATION SCHEME OF SACLA

SACLA is a hard x-ray FEL facility covering a photon energy range typically between 5–15 keV [2]. A schematic of the facility is shown in Fig. 1. SACLA employs normal-conducting high-gradient C-band accelerator structures (35–40 MV/m) and short-period variable-gap in-vacuum undulators to make the facility compact [8,9]. The undulator hall of SACLA is able to accommodate five undulator beam lines. In addition to these XFEL undulator beam lines, SACLA expects to be used as a low-emittance injector for the SPring-8 storage ring in future upgrade plans [10]. For the electron beam injection, a transport line called XFEL to synchrotron beam transport (XSBT), which branches from the undulator hall, was constructed.

*toru@spring8.or.jp
†Present address: Okinawa Institute of Science and Technology.

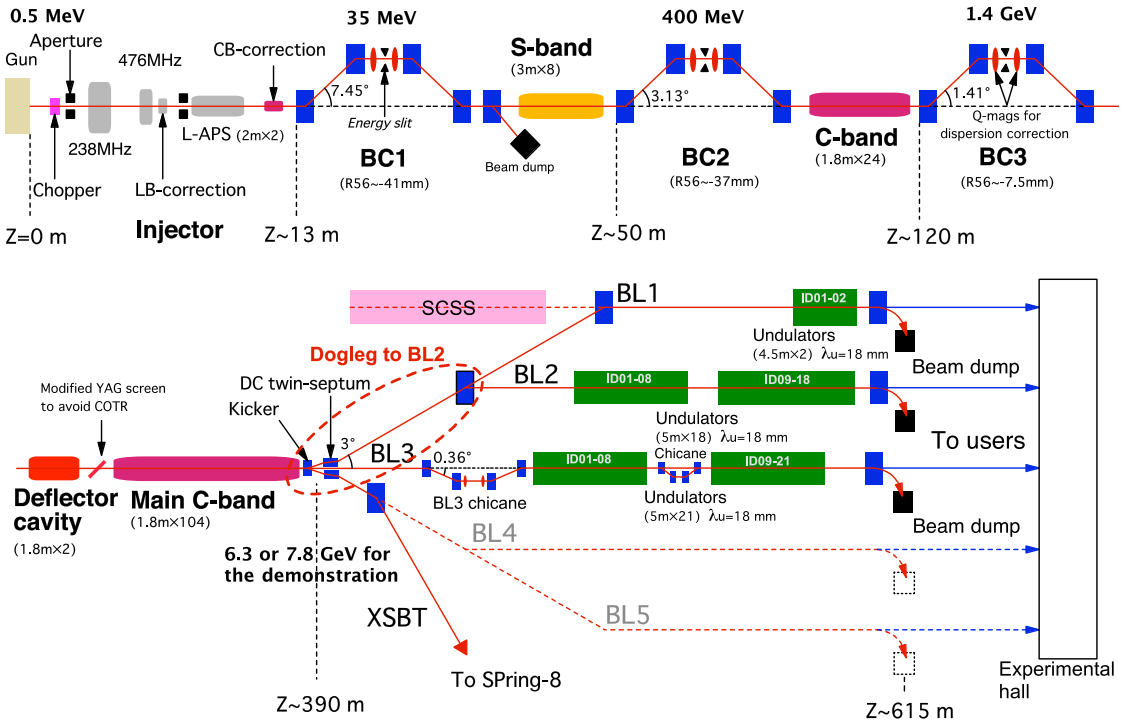

FIG. 1. Schematic of the SACLA facility.

A switchyard is located at the end of the accelerator, where the electron beam is deflected horizontally in three directions using a kicker magnet and a dc twin-septum magnet to switch between BL2, BL3 and XSBT. As shown in Fig. 1, the three directions, +3°, 0°, and −3°, correspond to BL2, BL3, and XSBT, respectively. BL3 is the first undulator beam line installed in the midst of the five beam lines, so the electron beam travels straight from the accelerator. BL2 is the second undulator beam line recently installed adjacent to BL3. The undulators of BL2 and BL3 have the same parameters with a periodic length of 18 mm.

When all undulator beam lines are placed downstream from the accelerator, tunability of photon wavelength becomes an issue for multi-beam-line operations. Although the wavelength can be adjusted to some extent with the undulator K-value, it is necessary to change the electron beam energy for a broad tuning range. At SACLA, a method to control the electron beam energy for individual bunches has been introduced so that the beam energies are optimized for the specific wavelengths of each beam line [6]. This multienergy operation of the linear accelerator allows for parallel operation of user experiments in different photon wavelength ranges.

III. BEAM LINE SWITCHING

The multi-beam-line operation was demonstrated using two undulator beam lines, BL2 and BL3. To transport the electron beam to BL2, the kicker and septum magnets first deflect the beam horizontally by +3°, and then another dc bending magnet deflects it back by −3° to make the beam orbit parallel to the BL3 undulators (Fig. 1). The electron beam optics and the magnet configuration for the beam transport to BL2 are shown in Fig. 2. The length of the dogleg part is about 65 m. The horizontal dispersion function is closed at the end of the dogleg in order to be achromatic. Two small bending magnets at the middle of the dogleg cancel R_{56} to prevent the change of the electron bunch length.

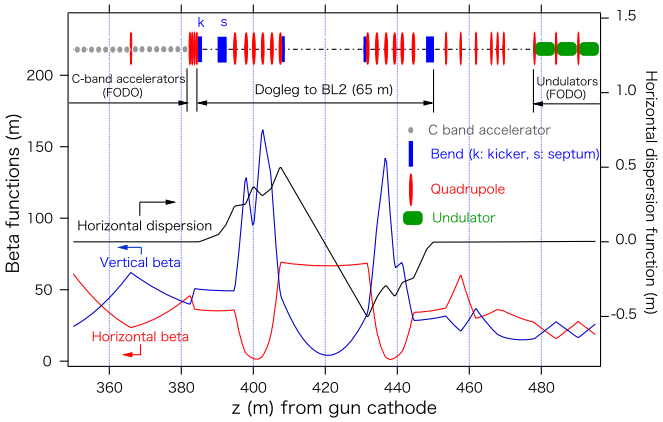

FIG. 2. Electron beam optics and magnet configuration for the beam transport from the end of the accelerator to the BL2 undulators. Solid lines indicate the horizontal beta function (red), vertical beta function (blue), and horizontal dispersion function (black), respectively. The inset on top shows the magnet configuration.

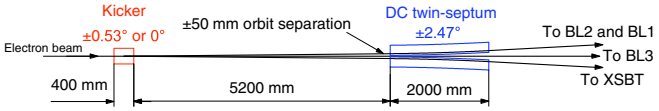

FIG. 3. Configuration of the beam line switchyard composed of kicker and dc twin-septum magnets located at the end of the linear accelerator.

Since electron beam orbit stability is vital for stable operation of an XFEL [11], 0.1 μrad (peak to peak) is set as the target stability for the kicker magnet. The deflection angle of the kicker ($\pm 0.53°$) is maintained as small as possible to relax the stability requirements for a pulsed power supply. The rest of the angle ($\pm 2.47°$) is provided by the dc twin-septum magnet placed 5.2 m downstream of the kicker, as shown in Fig. 3. Since the 3° deflection is unequally divided between the kicker and the septum magnet, symmetry is broken in the beam optics of the BL2 dogleg. Therefore, a double bend achromat (DBA) based lattice cannot be applied to cancel out the transverse CSR effects [12,13].

The length of the kicker is 0.4 m and its yoke is made with laminated silicon steel plates with a thickness of 0.35 mm. A ceramic vacuum duct is used at the magnetic gap (20 mm in height) to suppress eddy currents. The beam aperture of the ceramic duct is 33 mm (horizontal) and 10 mm (vertical). The dc twin-septum magnet is composed of two identical septum magnets placed symmetrically on the right and left sides. The magnets deflect the electron beam in opposite directions. To deliver the electron beam to BL3, the kicker magnet is turned off and the electron beam passes between the two septums.

The power supply for the kicker magnet is a nonresonant type and is able to output a bipolar, trapezoidal waveform of current with an arbitrary amplitude. The output current is regulated by pulse width modulation using eight FET units connected in parallel, as shown in Fig. 4. The 100 kHz switching cycle is synchronized with the timing clock of the accelerator to avoid current ripples. The target stability of the magnetic fields is 1×10^{-5} (peak to peak) from pulse to pulse.

The duration of a single trapezoidal waveform is 16.6 ms, corresponding to the maximum beam repetition of 60 Hz. The power supply can store up to four waveforms in a memory bank and the stored waveforms compose a switching pattern. Then the power supply controls and repeats the current output according to the switching pattern, for example as shown in Fig. 5. The arrival timing of the electron bunches to the kicker is set at the end of the flat top of the trapezoidal waveform, where the current output is well regulated and stabilized. By properly setting the amplitude and polarity of the waveforms, the electron bunches with different beam energies are delivered to the desired directions in the multienergy operation of the accelerator. In the case of Fig. 5, the switching pattern is composed of four waveforms, by which half of the electron bunches of 7 GeV are deflected to BL2, a quarter of the bunches of 6 GeV are sent to XSBT, and the last quarter of the bunches of 8 GeV go to BL3.

Before the installation, the stability and reproducibility of the kicker pulses were measured and checked by a dc current transformer (DCCT) and a gated nuclear magnetic resonance (NMR) detector [14]. Due to environmental noise, it was hard to measure the pulsed current with a relative resolution better than 10^{-5} using a DCCT. On the other hand, the measurements of pulsed magnetic fields with a gated NMR detector (Echo Denshi) attained a resolution of 2×10^{-6}. Different from conventional NMR detectors, a resonant frequency is scanned only when the gate is opened during 0.6 ms in the gated NMR detector. Thus the magnetic fields at the beam arrival timing could be accurately measured.

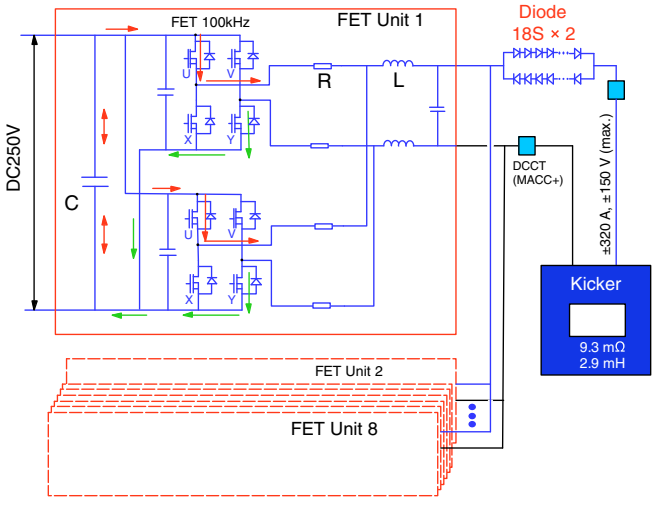

FIG. 4. Block diagram of the kicker magnet power supply. FET units are water cooled.

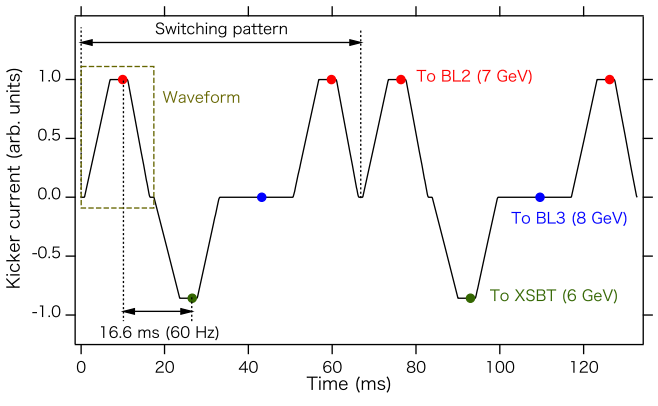

FIG. 5. An example of a switching pattern. Solid colored circles show the arrival timing of 60 Hz electron bunches. Half of the bunches, whose energy is 7 GeV, are deflected to BL2 (red circles). A quarter of them, having 6 GeV energy, are deflected to XSBT (green circles), and the rest of the bunches travel straight through the kicker magnet to BL3 with 8 GeV (blue circles).

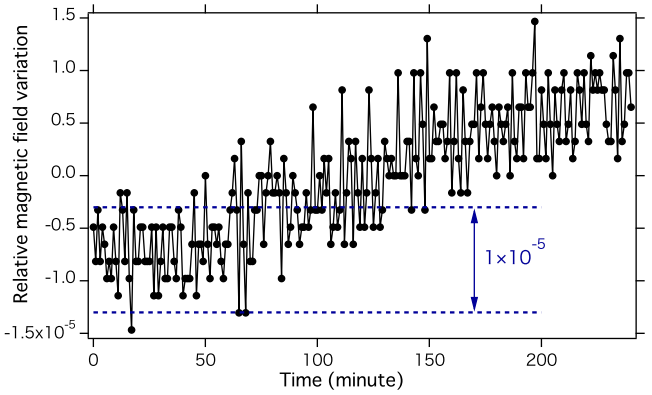

FIG. 6. Stability of the kicker magnetic fields measured by a gated NMR detector. The kicker magnet was operated at 60 Hz with a peak magnetic field of 0.61 T. The magnetic fields at the electron bunch arrival timing were measured and its relative variation was plotted with a sampling interval of one minute.

Figure 6 shows the measured stability and reproducibility of the pulsed magnetic fields. Except for a slow drift, pulse-to-pulse variation turned out to be about 1×10^{-5} (peak to peak), equivalent to an angular orbit error of 0.1 μrad, so the targeted stability was almost achieved. The temperature changes of the magnet and the power supply are mainly responsible for the slow drift, which becomes particularly significant after start-up or following the change of parameters. Since the time scale of the drift is tens of minutes, the resulting electron beam orbit errors can be corrected using a beam orbit feedback system.

IV. MULTI-BEAM-LINE OPERATION

The commissioning of the second undulator beam line, BL2, first began with high peak current bunches around 10 kA used for the normal operation of BL3 (Fig. 7, "high peak current"). Although laser light was successfully

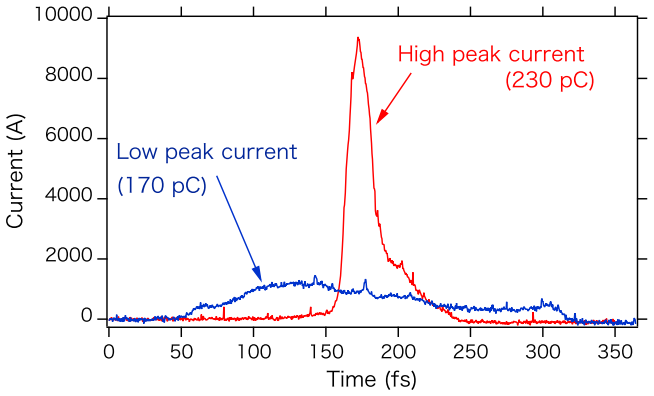

FIG. 7. Longitudinal current profiles of the electron bunch measured by a C-band rf deflector [15]. The profile shown in red is the electron bunch with a high peak current used for the normal operation of BL3. The profile shown in blue is the electron bunch with a low peak current obtained after parameter optimization for BL2.

observed, its intensity fluctuated strongly and the pulse energy stayed around 30 μJ, which is an order of magnitude smaller than the nominal values obtained at BL3. The transverse electron beam profiles inside the undulators were horizontally distorted and its position varied randomly from pulse to pulse.

In order to pursue higher photon pulse intensity, the peak current of the electron bunches has been increased at SACLA and it currently reaches nearly 10 kA, more than 3 times higher than the original design value [16]. Consequently, laser pulses estimated to be less than 10 fs (FWHM) by a single-shot spectrometer [17] are now available for user experiments.

Short electron bunches and photon pulses are preferable for user experiments, particularly for dynamical observations of phenomena. However short electron bunches with a high peak current impose a severe condition on beam transport, because they provoke significant distortion of the electron distribution in time-energy phase space due to the CSR effects as they pass through bending magnets [18–20]. The main component of the CSR fields is longitudinal, which modulates the electron energy inside the bunch. The change of the electron energy inside an achromatic dogleg results in projected emittance growth, which is analogous to the chromatic effect of nonzero dispersion. An increase of projected emittance leads to a decrease in the number of electrons contributing to the XFEL process. In a similar way, the electron energy change in an isochronous dogleg also distorts the shape and length of the electron bunch. The distortion of the longitudinal bunch shape can cause an increase in slice emittance, resulting in further reduction of XFEL gain.

In order to increase the XFEL output from BL2, an optimum condition of operation was searched. In addition to transverse envelope matching conditions, the peak current of the electron bunch was varied. As reducing the peak current, the fluctuations of the electron beam orbit and the laser pulse intensity became smaller, and the transverse electron beam profiles approximated a round shape. Finally around 1 kA of the peak current (Fig. 7, "low peak current"), the maximum intensity of 100–150 μJ was obtained with an undulator K-value of 2.85.

TABLE I. Measured stability of the injection orbit to the undulators. Both position and angle were measured and the area (rms) of distribution in the phase space was calculated for the horizontal and vertical planes. The electron bunch profiles for the high and low peak currents are shown in Fig. 7. The beam energy was 7.8 GeV.

BL and condition	Horizontal plane (pm-rad)	Vertical plane (pm-rad)
BL2, high peak current	16.3	0.74
BL2, low peak current	2.7	0.64
BL3, high peak current	1.4	0.27
BL3, low peak current	0.83	0.24

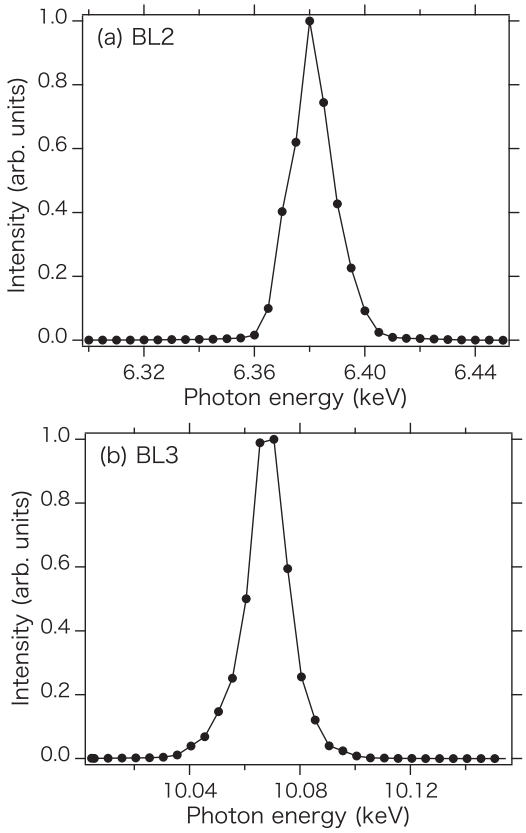

FIG. 8. Averaged laser spectra measured by scanning a monochromator in the multi-beam-line operation, (a) BL2 and (b) BL3. The electron beam energy was 7.8 GeV and the undulator K-values were 2.85 and 2.1 for BL2 and BL3, respectively. The peak current is 1.2 kA for both beam lines.

Table I summarizes the orbit stability of the electron beam measured by two beam position monitors located upstream of the undulators. The increase in the horizontal fluctuation for the high peak current at BL2 was mainly due to the CSR effects. Even for BL3, to which the electron beam travels straight from the accelerator end, we still saw a slight increase, which was probably due to the wakefields of the accelerator structures and the CSR effects at the bunch compressors and a chicane in front of BL3. Although the fluctuation of BL2 was always larger than that of BL3, it reduced to an acceptable range with the low peak current bunches. Assuming a normalized emittance of 0.8 μm-rad and a beam energy of 7.8 GeV, the orbit fluctuation of the low peak current at BL2 was less than 10% of the electron beam emittance size, which is 52 pm-rad.

After optimizing the electron beam parameters for BL2, the multi-beam-line operation was tested using the electron bunches of the low peak current around 1.2 kA. The repetition of the electron bunches from the accelerator was 30 Hz and all the bunches were accelerated to 7.8 GeV. BL2 and BL3 were alternately switched by the kicker magnet. Figure 8 shows the laser spectra measured at the two beam lines. The photon energies obtained at BL2 and BL3

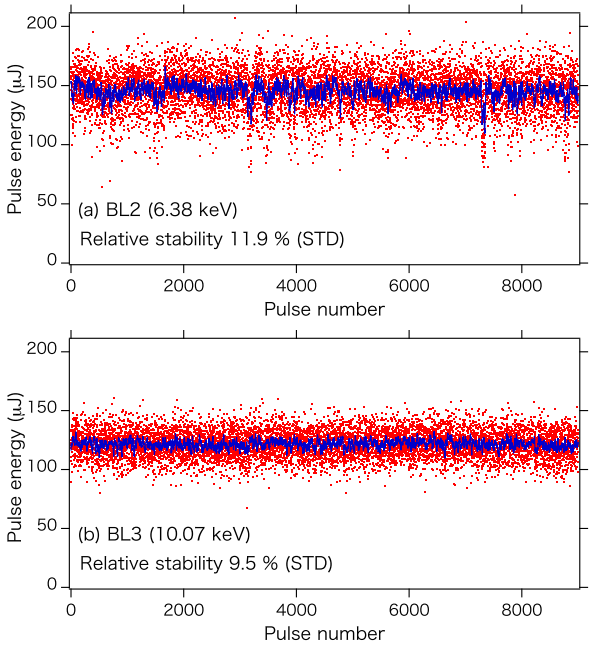

FIG. 9. Stability of the photon pulse intensity measured by an intensity monitor [21] in the multi-beam-line operation, (a) BL2 and (b) BL3. Red points represent single-shot results and blue lines show averaged values over 15 shots. The pulse repetition at each beam line was 15 Hz and the full horizontal scale corresponds to 10 minutes. The electron beam energy was 7.8 GeV and the undulator K-values were 2.85 and 2.1 for BL2 and BL3, respectively. The peak current is 1.2 kA for both beam lines.

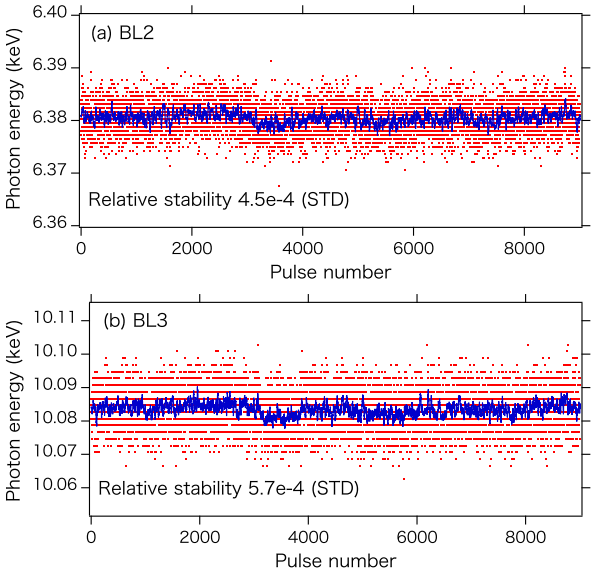

FIG. 10. Stability of the central photon energy measured by a wavelength monitor [22] in the multi-beam-line operation, (a) BL2 and (b) BL3. Red points represent single-shot results and blue lines show averaged values over 15 shots. The pulse repetition at each beam line was 15 Hz and the full horizontal scale corresponds to 10 min. The electron beam energy was 7.8 GeV and the undulator K-values were 2.85 and 2.1 for BL2 and BL3, respectively. The peak current is 1.2 kA for both beam lines.

were 6.38 and 10.07 keV with $K = 2.85$ and $K = 2.1$, respectively. The stabilities of the laser intensity and the central photon energy were also measured, as shown in Figs. 9 and 10. Stable operation of XFEL was achieved at both beam lines.

Fixing the electron beam energies the same for the two beam lines eventually imposes a limitation in wavelength tunability. In order to remove this limitation, the multienergy operation of the accelerator was applied [6]. At SACLA, there are 52 C-band units (klystrons) downstream from the third bunch compressor. In single-energy operation, all klystrons run at 30 Hz, which is the same as the electron bunch repetition. But in multienergy operation, some of the klystrons are operated at half the bunch repetition, i.e., 15 Hz. Then half of the electron bunches are not accelerated in the accelerator structures powered by these klystrons.

In the demonstration, 12 C-band units were operated at 15 Hz to lower the beam energy to 6.3 GeV for BL2, while the beam energy for BL3 was maintained at 7.8 GeV. The peak current is 1.2 kA. Figure 11 shows the spectra measured at the two beam lines. By decreasing the beam energy of BL2, the photon energy range was extended to 4.09 keV, more than 2 times different than that of BL3. The stability of the laser intensity is plotted in Fig. 12. Compared to Fig. 9, no degradation of the laser stability was observed in the multienergy operation of the accelerator.

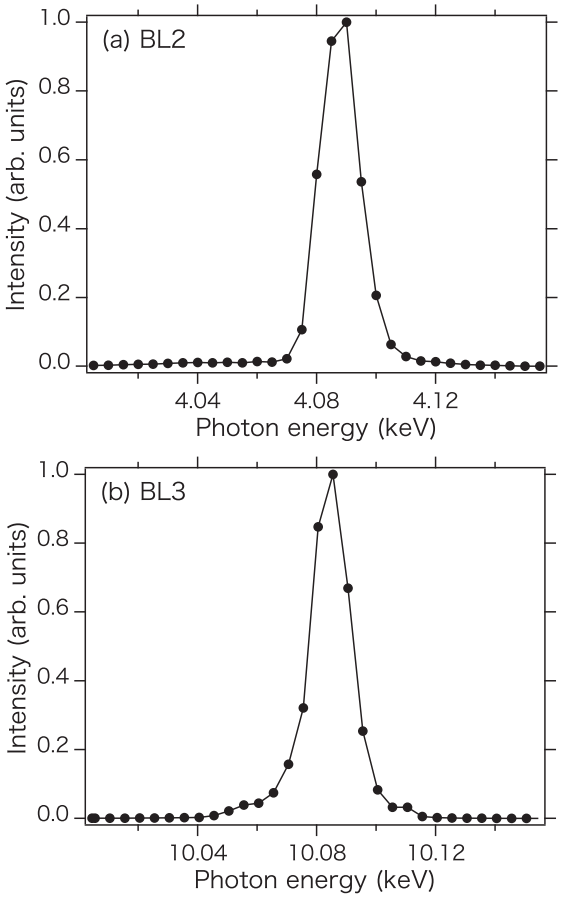

FIG. 11. Averaged laser spectra measured by scanning a monochromator in the multi-beam-line operation combined with the multienergy operation of the accelerator, (a) BL2 and (b) BL3. The electron beam energy of BL2 was 6.3 GeV and that of BL3 was 7.8 GeV. The undulator K-values were 2.85 and 2.1 for BL2 and BL3, respectively. The peak current is 1.2 kA for both beam lines.

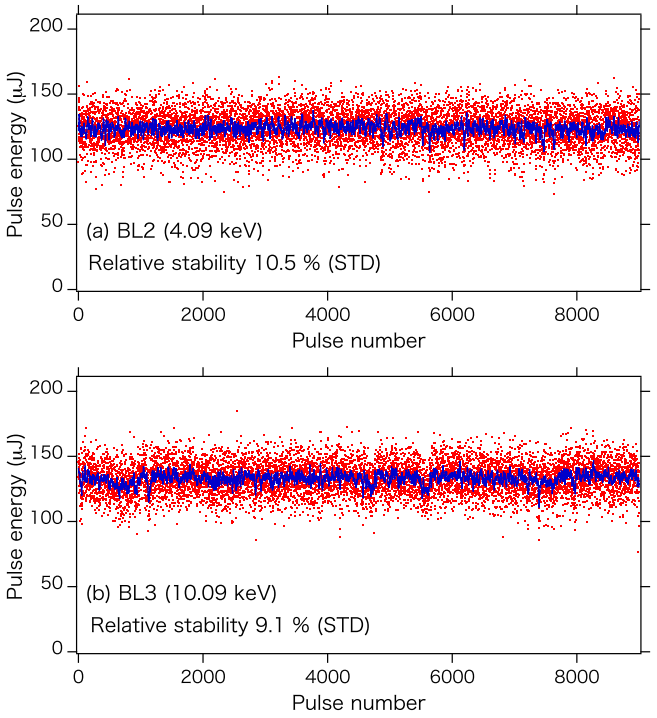

FIG. 12. Stability of the photon pulse intensity measured by an intensity monitor in the multi-beam-line operation combined with the multienergy operation of the accelerator, (a) BL2 and (b) BL3. Red points represent single-shot results and blue lines show averaged values over 15 shots. The pulse repetition at each beam line was 15 Hz and the full horizontal scale corresponds to 10 minutes. The electron beam energy of BL2 was 6.3 GeV and that of BL3 was 7.8 GeV. The undulator K-values were 2.85 and 2.1 for BL2 and BL3, respectively. The peak current is 1.2 kA for both beam lines.

V. DISCUSSIONS

The multi-beam-line operation at SACLA demonstrates how to increase the capacity of user experiments at XFEL facilities. To obtain wavelength tunability over a broad spectral range, the beam energies of individual bunches can be controlled and optimized for the wavelengths of each beam line. This multienergy operation allows the sharing of the electron beam in multi-beam-line operation at compact XFEL facilities.

The CSR effects observed at the dogleg currently limit the peak current of the electron bunch for BL2. As a result,

the laser pulse intensity of BL2 remains around 100–150 μJ. For higher laser intensity, it is necessary to increase the peak current and to suppress the CSR effects. The present beam optics of the dogleg assumes the 3 kA bunch of the original design, and it does not take into account the cancellation of the CSR effects. To cancel out the transverse CSR effects, rearrangement of the beam optics at the dogleg is currently being investigated. In the new optics, four identical bending magnets, whose deflection angle is 1.5°, are used, and the horizontal phase advance between the magnets is kept as π [12,13]. Assuming a 10 kA-10 fs (rms) Gaussian beam with 0.8 μm-rad normalized emittance, the horizontal emittance of 0.82 μm-rad is obtained after the dogleg for the new optics compared to 9.4 μm-rad for the current optics in the simulations.

For an injector of the upgraded SPring-8 storage ring, switching at arbitrary timing is required for sharing the electron beam between the XFEL beam lines and the beam injection. For this purpose, not only the beam energy but also the bunch length must be controlled from pulse to pulse. To satisfy these requirements, the development of a new low-level rf and timing system is under way.

ACKNOWLEDGMENTS

The authors wish to acknowledge the support of the SACLA team, for their help with the accelerator operations and the data acquisition.

[1] P. Emma *et al.*, Nat. Photonics **4**, 641 (2010).
[2] T. Ishikawa *et al.*, Nat. Photonics **6**, 540 (2012).
[3] V. Balandin, W. Decking, and N. Golubeva, in *Proceedings of the 2nd International Particle Accelerator Conference, San Sebastián, Spain* (EPS-AG, Switzerland, 2011), p. 2016.
[4] J. H. Han, H. S. Kang, and I. S. Ko, in *Proceedings of the 3rd International Particle Accelerator Conference, New Orleans, LA, 2012* (IEEE, Piscataway, NJ, 2012), p. 1735.
[5] S. Reiche, in *Proceedings of the 33rd Free Electron Laser Conference, Shanghai, China* (EPS-EG, Switzerland, 2011), p. 223.
[6] T. Hara *et al.*, Phys. Rev. ST Accel. Beams **16**, 080701 (2013).
[7] R. Talman, Phys. Rev. Lett. **56**, 1429 (1986).
[8] T. Inagaki, C. Kondo, H. Maesaka, T. Ohshima, Y. Otake, T. Sakurai, K. Shirasawa, and T. Shintake, Phys. Rev. ST Accel. Beams **17**, 080702 (2014).
[9] T. Tanaka, S. Goto, T. Hara, T. Hatsui, H. Ohashi, K. Togawa, M. Yabashi, and H. Tanaka, Phys. Rev. ST Accel. Beams **15**, 110701 (2012).
[10] H. Tanaka, Synchrotron Radiat. News **27**, 23 (2014).
[11] T. Tanaka, H. Kitamura, and T. Shintake, Phys. Rev. ST Accel. Beams **5**, 040701 (2002).
[12] D. Douglas, Thomas Jefferson National Accelerator Facility Report No. JLAB-TN-98-012, 1998.
[13] S. Di Mitri, M. Cornacchia, and S. Spampinati, Phys. Rev. Lett. **110**, 014801 (2013).
[14] T. Hara *et al.*, in *Proceedings of the 36th Free Electron Laser Conference, Bazel, Switzerland* (JACoW, Switzerland, 2014), p. 71.
[15] H. Ego, H. Maesaka, T. Sakurai, Y. Otake, T. Hashirano, and S. Miura, Nucl. Instrum. Methods Phys. Res., Sect. A **795**, 381 (2015).
[16] T. Hara, K. Togawa, and H. Tanaka, in *Proceedings of the 32nd Free Electron Laser Conference, Malmö, Sweden* (Max-lab, Sweden, 2010), p. 111.
[17] Y. Inubushi *et al.*, Phys. Rev. Lett. **109**, 144801 (2012).
[18] B. E. Carlsten and T. O. Raubenheimer, Phys. Rev. E **51**, 1453 (1995).
[19] M. Dohlus and T. Limberg, Nucl. Instrum. Methods Phys. Res., Sect. A **393**, 494 (1997).
[20] E. L. Saldin, E. A. Schneidmiller, and M. V. Yurkov, Nucl. Instrum. Methods Phys. Res., Sect. A **398**, 373 (1997).
[21] K. Tono, T. Kudo, M. Yabashi, T. Tachibana, Y. Feng, D. Fritz, J. Hastings, and T. Ishikawa, Rev. Sci. Instrum. **82**, 023108 (2011).
[22] K. Tono *et al.*, New J. Phys. **15**, 083035 (2013).